CHAPTER FOUR:

UNDERSTANDING N-TYPE VOLTAGE-GATED CALCIUM CHANNEL MOBILITY AND INTERACTION WITH SYNTAXIN-1A.

4.1 Introduction

The exocytosis process is mediated by SNARE proteins. Membrane fusion is driven by zippering of the SNARE helix from VAMP-2, two SNARE helices from SNAP-25 and one from syntaxin-1 thus creating the four-helix bundle structure[43]. This interaction is thought to require specific binding of SNAP-25 and syntaxin-1A to a synprint site motif at the intracellular loop of the α_{1B} subunit N-type calcium channel[45,27]. Although the research indicates the synaptic protein interaction site is essential for fast and effective exocytosis, their distribution with each other has never been identified.

In this chapter, I aim to analyse the interaction of N-type calcium channels with syntaxin-1A using FLIM-FRET and STORM methods.

It is hypothesised that the mobility of calcium channels will have an impact on vesicle fusion. Therefore, the lateral mobility of N-type calcium channels at the cell membrane was assessed using the Cav2.2 splice variant without synprint site motif and the response compared to that observed for the full-length Cav2.2 calcium channels.

4.2 FLIM-FRET measurement of the interaction between N-type calcium channels and syntaxin-1A

To determine N-type calcium channel and syntaxin-1A interaction, the FLIM-FRET[139] method was used. Fluorescence lifetime imaging microscopy can be used to measure the Förster Resonance Energy Transfer between two proteins in close proximity <10 nm[139] (described in Chapter 1.4.7). To verify the acquisition and analysis method, a control examination was performed. The fluorescence lifetimes and FRET efficiencies were compared between EGFP, EGFP co-expressed with mCherry and EGFP fused to mCherry expressed in the PC12 cells. Images were acquired by using a Leica SP5 SMD CLSM microscope equipped with Picoharp 300 TCSPC module and single photon avalanche diode (SPAD) detectors for fluorescence lifetime imaging. Analysis of FLIM was done by using SymPhoTime v5.4.4 (PicoQuant). To determine the pixel FRET efficiencies, a Microsoft Excel VBA script designed by Dr Rebecca Saleeb (Institute of Biological Chemistry, Biophysics and Bioengineering, Heriot-Watt University, Edinburgh) was used. The results

from this control are experiments presented in figure 4.1. As expected there is a decrease in fluorescence lifetime in the fused construct (figure 4.1a, c). In comparison to EGFP, the median fluorescence lifetime of EGFP fused to mCherry decreased 17.2%, from 2.17 ns to 1.78 ns (figure 4.1c). The EGFP median fluorescence lifetime co-expressed with mCherry was 1.99 ns which is 8.3% lower than only EGFP (figure 4.1c). The FRET efficiency histogram indicates those differences (figure 4.1b). EGFP fused to mCherry has distribution right-shifted with the comparison to the EGFP and to the EGFP co-expressed with mCherry. This change in FRET efficiency indicates the interaction of EGFP and mCherry (figure 4.1b).

Next, Cav2.2-EGFP calcium channels were expressed in PC12 as a donor and immunolabeled with primary antibody anti-syntaxin-1A (HPC-1) (monoclonal mouse, Sigma) and secondary antibody monoclonal anti-mouse Alexa Fluor 568 (Thermo Fisher), as an acceptor. The results are presented in figure 4.2. There are no changes in fluorescence lifetime for Cav2.2 in a presence of acceptor. The median fluorescence lifetime for the donor and acceptor is 1.89 ns (figure 4.2c). The FRET efficiency distribution close to 0 indicates no differences (figure 4.2b).

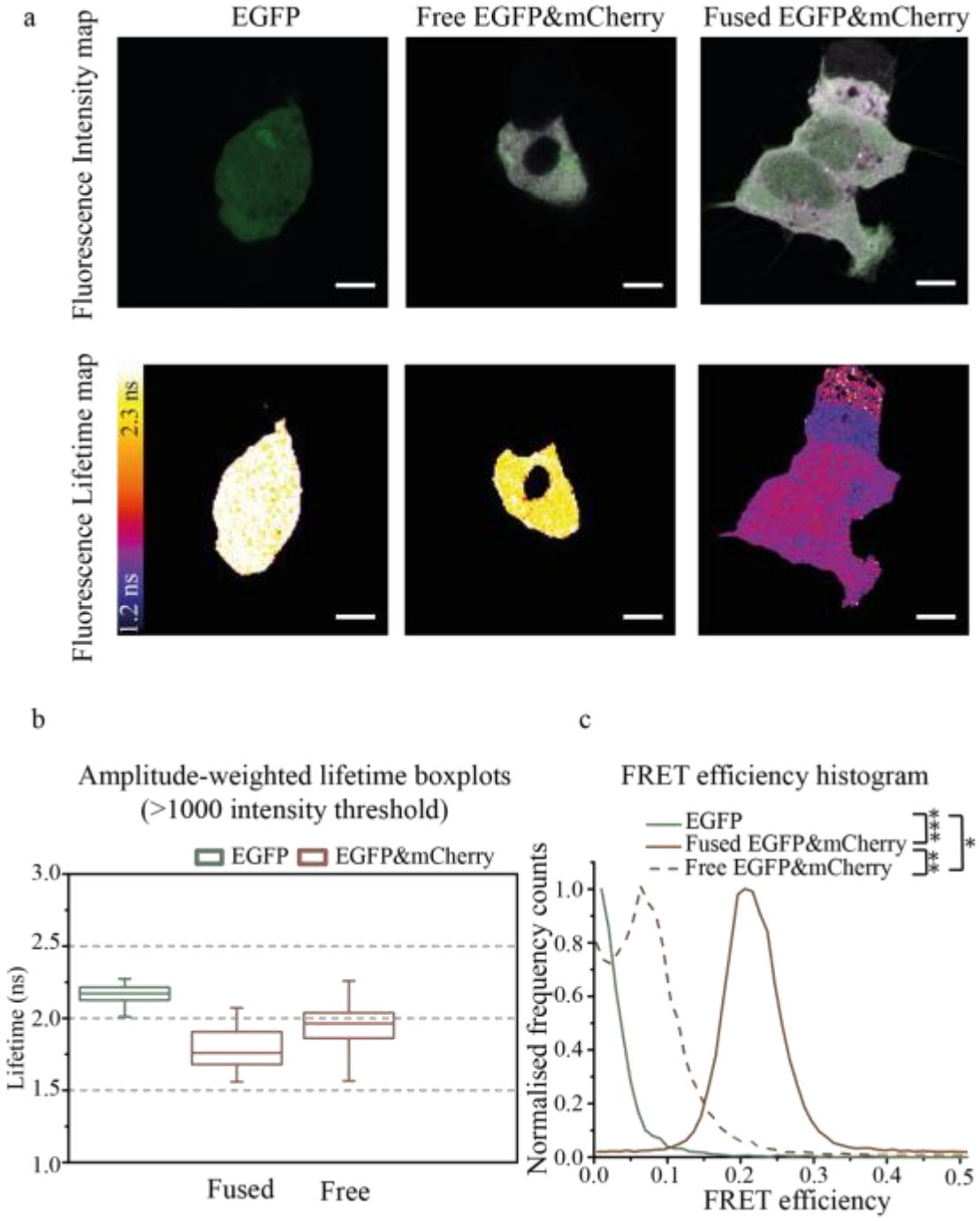

Figure 4.1 FLIM-FRET verification of fused EGFP and mCherry. PC12 cells were transfected with EGFP, EGFP co-expressed with mCherry (free) and EGFP fused to mCherry. (a) Fluorescence intensity images and fluorescence amplitude-weighted lifetime maps. (scale bar 5 µm) (b) Box-and-whisker plots of the amplitude-weighted lifetime. The centre line indicates median value, the boxes 25th and 75th quartile values, and whiskers min and max values. To determine statistical significance the non-parametric Kruskal-Wallis test was used. (c) FRET efficiency histogram indicates those changes. The EGFP fused to mCherry has right shifted distribution. Number of cells =3.

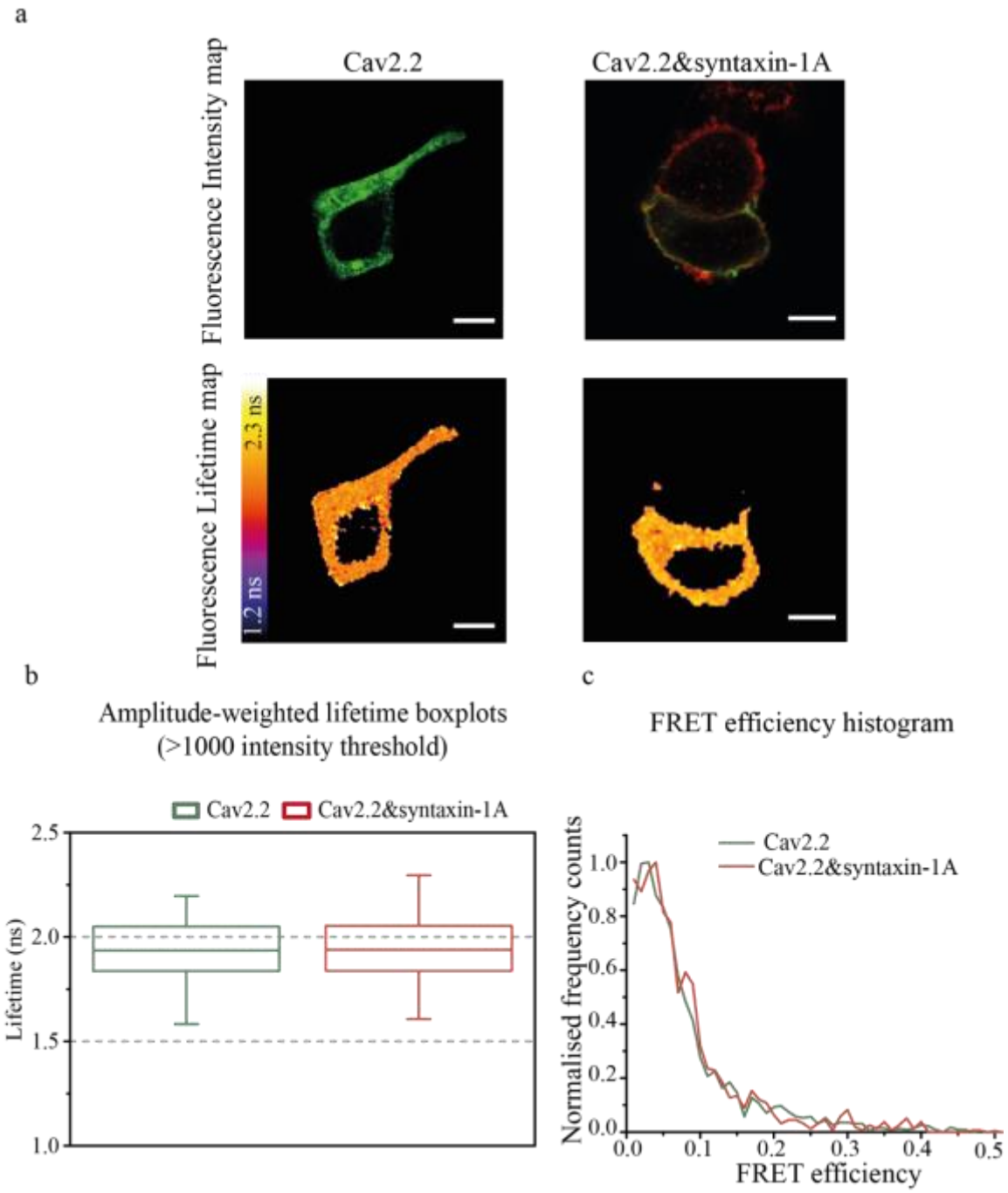

Figure 4.2 FLIM-FRET measurement of interaction between Cav2.2 and syntaxin-1. PC12 cells were transfected with Cav2.2-EGFP and immunolabelled with syntaxin-1A-AlexaFluor568. (a) Fluorescence intensity images and fluorescence amplitude-weighted lifetime maps. (scale bar 5 µm) (b) Box-and-whisker plots of the amplitude-weighted lifetime. The centre line indicates median value, the boxes 25th and 75th quartile values, and whiskers min and max values. To determine statistical significance the non-parametric Mann-Whitney U test was used. (c) FRET efficiency histogram indicates distribution close to 0 for both. Number of cells =3.

4.3 Molecular architecture of syntaxin-1A relative to N-type calcium channels using dSTORM

To determine the molecular organisation of syntaxin-1A in relation to N-type calcium channels, nearest neighbour analysis was performed. Full-length and the splice-variant Cav2.2 calcium channel were expressed, fused to EGFP in the PC12 cells and syntaxin-1A (HPC-1) was immunolabeled with Alexa Fluor 647. The cells were imaged with the Olympus IX-81 microscope using direct stochastic optical reconstruction microscopy (dSTORM)[116] in TIRF mode. The Matlab script for nearest neighbour analysis[75] was written by Dr Colin Rickman (Institute of Biological Chemistry, Biophysics and Bioengineering, Heriot-Watt University, Edinburgh). Using the coordinate data describing syntaxin-1A and the centre coordinates of diffraction-limited Cav2.2 clusters, syntaxin-1A molecules were allocated to their nearest Cav2.2 calcium channel cluster (figure 4.3b, c). The number of syntaxin-1A molecules within N-type calcium channel cluster radii were analysed for full-length Cav2.2 and splice Cav2.2(Δ18a) (figure 4.4). For analysis, three different radius size of N-type calcium channels clusters were chosen. According to the Rayleigh criterion[98] of the lateral resolution of the microscope, for GFP and NA=1.4 the resolution is equal to 222 nm. Assuming the size of the cluster is 222 nm, the number of molecules within a radius of 111 nm was calculated (figure 4.4a). The second size of the cluster was chosen according to the size of clusters measured by gSTED, described in chapter 3.3. Relative to the mean size of N-type calcium channels cluster which is 125 nm, the radius of 62.5 nm was chosen (figure 4.4b). The final tested radius of calcium channel clusters was selected based on Bayesian analysis of PALM data (chapter 3.4.1). The mean size of clusters for PC12 cells, analysed with Bayesian cluster analysis is 50 nm, accordingly, the radius 25 nm was chosen (figure 4.4c). The number of syntaxin-1A molecules within N-type calcium channel cluster is presented in histograms in figure 4.4. The numbers of molecules within N-type calcium channel clusters varies between 0 and 21 (figure 4.4d). The average number of syntaxin-1A molecules in close proximity, below 25 nm to the N-type calcium channels is zero. The number of molecules increases with the size of the distance as would be expected. To check the difference between the number of molecules for full-length and splice variant, the non-parametric Mann-Whitney U test was used. There is a significant difference for 25 nm, 62.5 nm and 104.5 nm distance (figure 4.4d). The number of molecules is lower for splice variant Cav2.2(Δ18a) (figure 4.4).

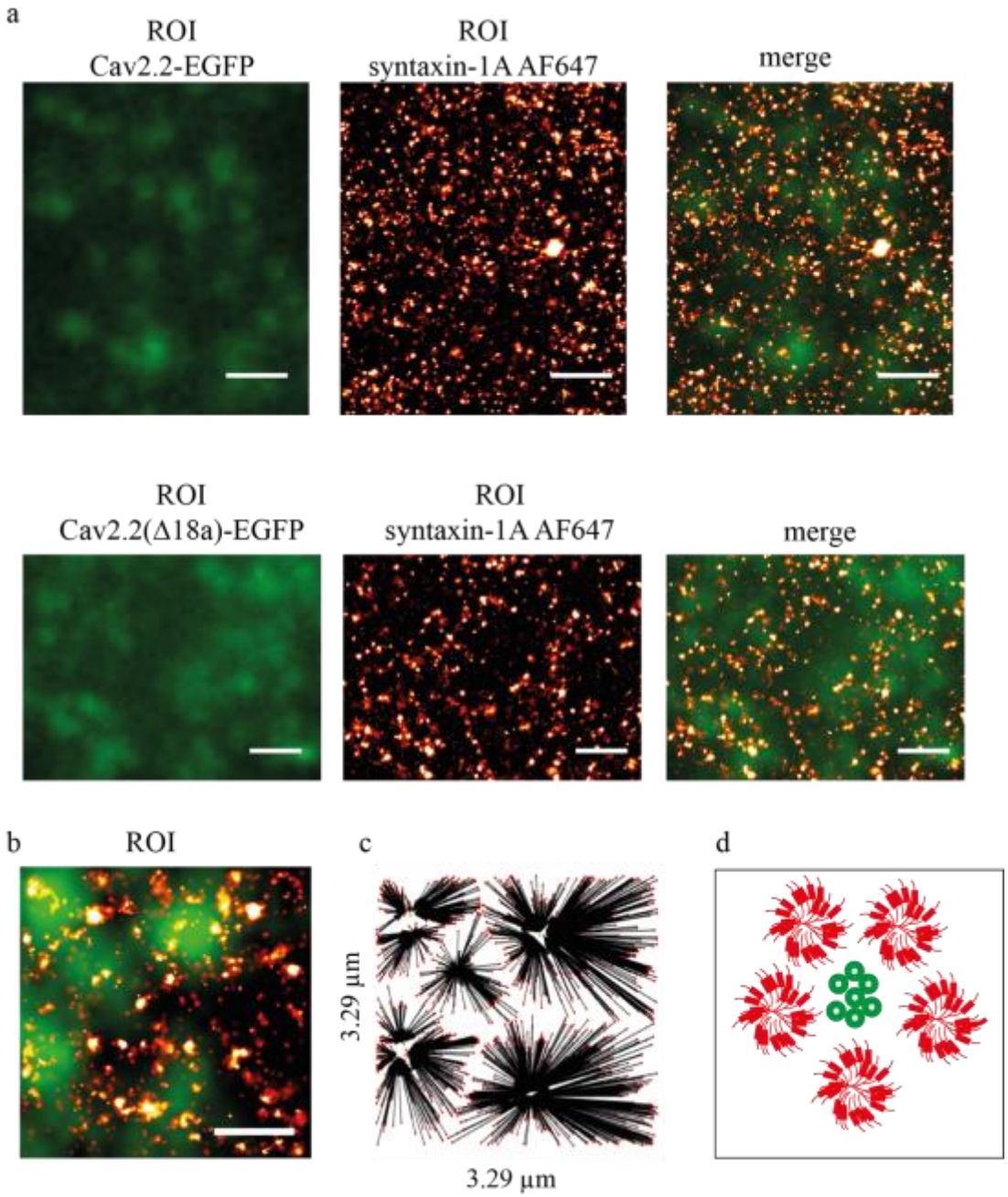

Figure 4.3 Nearest neighbour analysis of dSTORM images. (a) TIRF images of the region of interests created by summation of all detected Cav2.2 / Cav2.2(Δ18a) – EGFP signals (left), dSTORM of immunolabelled syntaxin-1A- AF647 molecules and rendered (centre) and merged (left) scale bar 1 µm. (b) Region showing merged of TIRF Cav2.2-EGFP and rendered dSTORM syntaxin-1A (scale bar 1 µm). (c) Centre of each Cav2.2 cluster was estimated and used in nearest neighbour analysis. (d) Distribution model of syntaxin-1A (red), calcium channels (green) (not to scale).

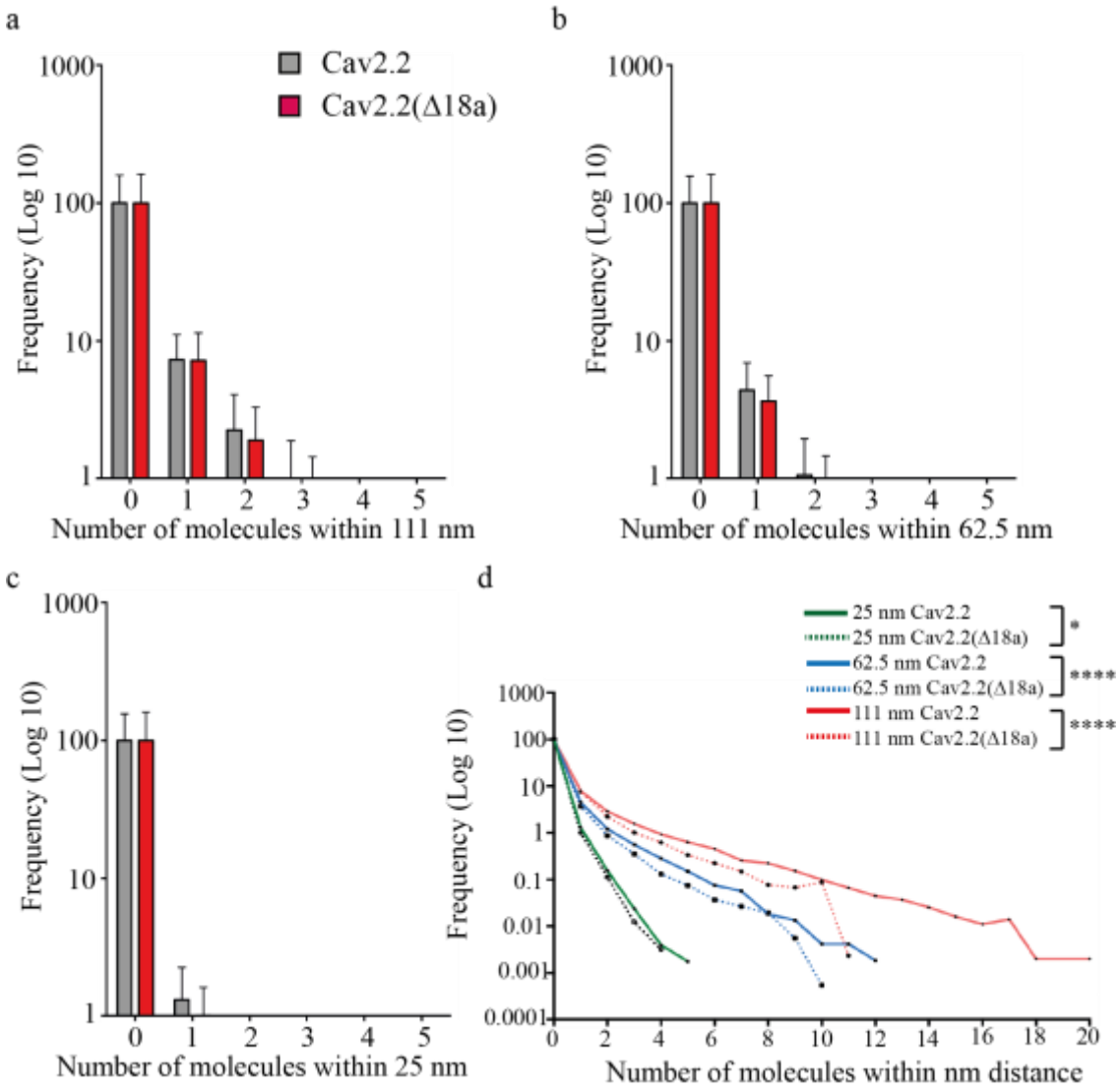

Figure 4.4 The numbers of syntaxin-1A molecules within Cav2.2 calcium channel cluster. The number of syntaxin-1A molecules within three different radii of Cav2.2 calcium channel clusters were analysed. (a) 111 nm radii based on microscopy resolution. (b) 62.5 nm based on gSTED cluster size and (c) 25 nm based on the Bayesian analysis. (d) Comparison of the number of syntaxin- 1A molecules for each radius. The non-parametric Mann - Whitney U test was used (* is $p = 0.0450$, **** is $p < 0.0001$).

4.4 Characterisation of the N-type calcium channels lateral mobility using sptPALM

To determine the mobility of N-type calcium channels, single particle tracking PALM was used. The full-length and splice variant of Cav2.2-PAmCherry calcium channels were expressed in HEK293 and PC12 cells. Over 4,000 frames were registered and analysed in Matlab with particle tracking software[170] written by Isabel Schlangen (Institute of Biological Chemistry, Biophysics and Bioengineering, Heriot-Watt University, Edinburgh). The results for HEK293 cells are presented in figure 4.5 and 4.6. The data does not fit to a normal distribution, so the median value of speed was compared. The non-parametric Mann-Whitney U test was used to compared each speed value (figure 4.6). The results indicate the N-type calcium channels without synprint motif are more static than full-length N-type calcium channels. The median value of average speed is lower, 0.25 $\mu m \cdot s^{-1}$, while for Cav2.2 is 0.27 $\mu m \cdot s^{-1}$ (figure 4.5b). The median minimum speed for Cav2.2 is 0.05 $\mu m \cdot s^{-1}$ while for the Cav2.2(Δ18a) higher 0.06 $\mu m \cdot s^{-1}$; effectively static, or below the limit of sensitivity for this assay. The difference in maximum speed can be also indicated. The median speed for Cav2.2 is 0.67 $\mu m \cdot s^{-1}$ and for the Cav2.2(Δ18a) is lower, 0.61 $\mu m \cdot s^{-1}$.

Similar results are presented for PC12 cells. The median average speed of Cav2.2 with synprint motif is higher, 0.28 μm·s-1 with minimum 0.05 μm·s-1 and maximum speed 0.70 μm·s-1 (figure 4.7). The Cav2.2 without synprint site are moving with lower speed. The median average speed 0.25 μm·s-1 (figure 4.7b) while the minimum is 0.06 μm·s-1 and maximum 0.59 μm·s-1.These results indicate the N-type calcium channels without synprint motif expressed in PC12 cells are also less mobile.

a

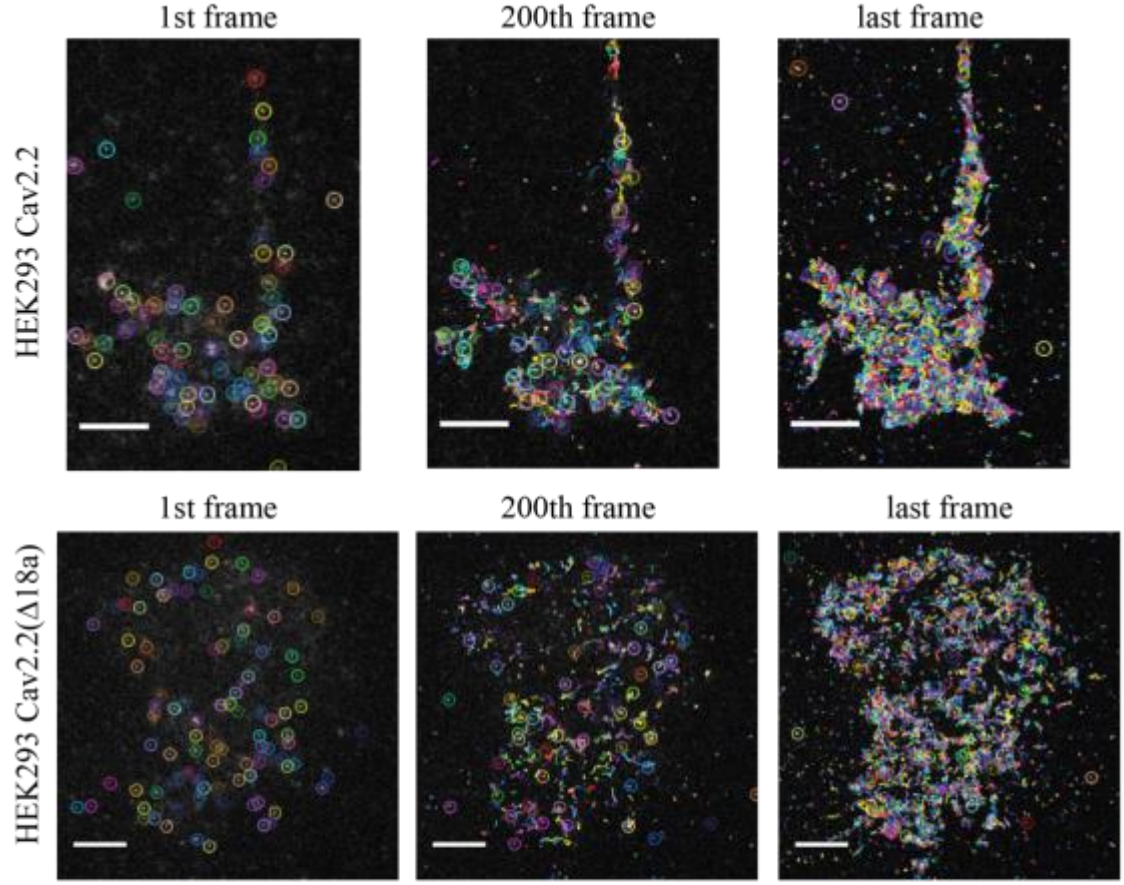

b

	Average speed (µm·s-1)		Min speed (µm·s-1)		Max speed (µm·s-1)	
	Cav2.2	Cav2.2(Δ18a)	Cav2.2	Cav2.2(Δ18a)	Cav2.2	Cav2.2(Δ18a)
Nr of cells	5	5	5	5	5	5
Nr of tracks	34745	44161	34745	44161	34745	44161
Minimum	3.332×10-5	6.392×10-6	2.192×10-5	1.278×10-5	6.663×10-5	1.278×10-5
Median	0.267	0.249	0.050	0.055	0.667	0.610
Maximum	2.637	3.288	0.687	0.559	5.997	12.410
Mean	0.301	0.289	0.058	0.063	0.738	0.695
SD	0.236	0.241	0.041	0.044	0.576	0.580

Figure 4.5 Single particle tracking of N-type calcium channels in HEK293 cells. (a) Cav2.2/Cav2.2(Δ18a) calcium channels were expressed with PACherry in HEK293 cells and analysed in Matlab with particle tracking software written by I. Schlangen. Images represent the detection in the 1st frame following with the tracking in the 200th and last frame. Each colour represents different particle (scale bar 5 µm) (b) Table with results of average, min and max speed for full-length (Cav2.2) and splice (Cav2.2(Δ18a)) calcium channels variant. Total number of frames = 4,000.

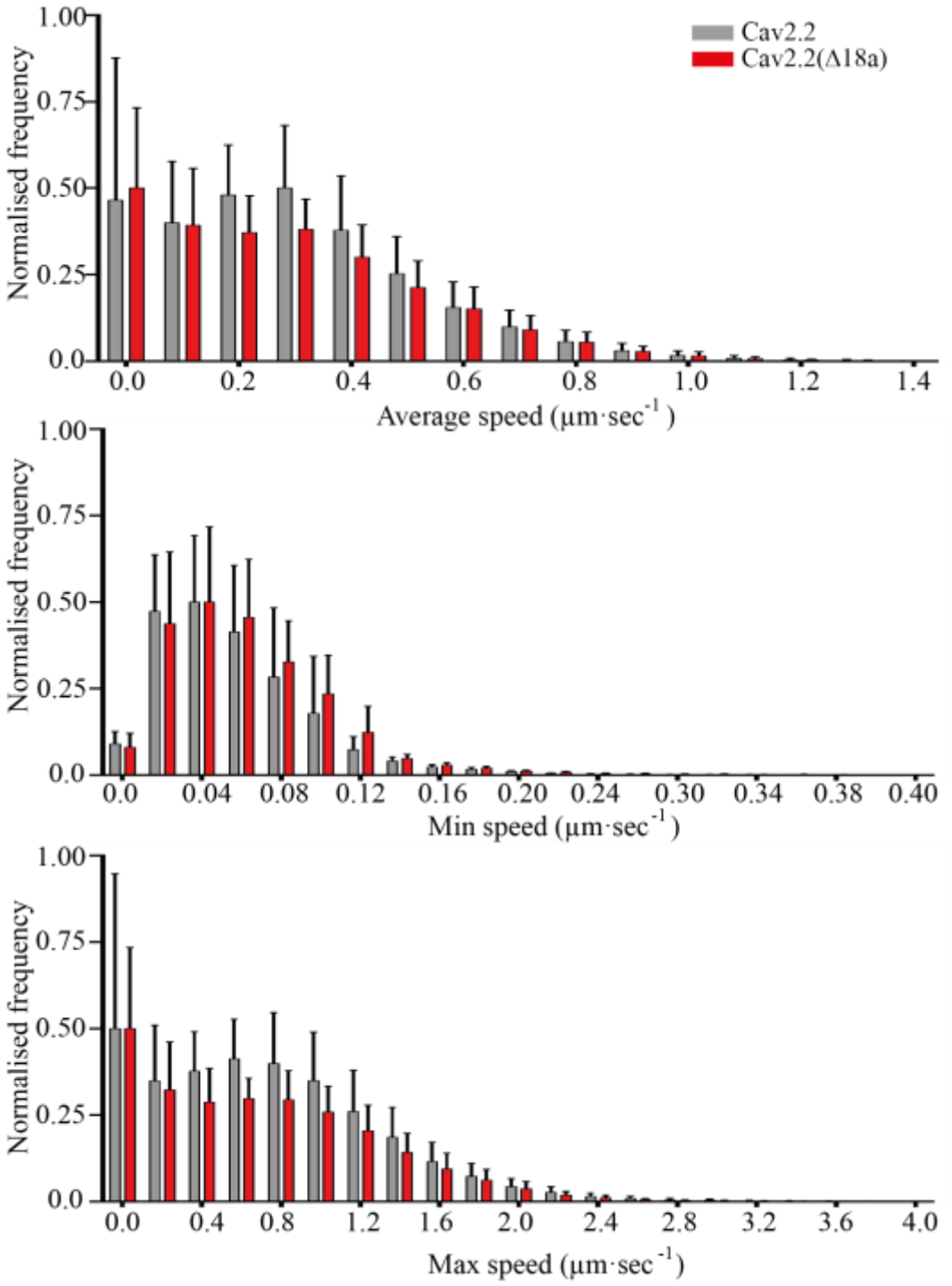

Figure 4.6 The mobility of N-type calcium channels in HEK293 cells. Combined average, min and max speed for each individual N-type calcium channel presented as the normalized frequency histogram of mean ± SD (number of tracks 34745 for Cav2.2, 44161 for Cav2.2(Δ18a)). The non-parametric Mann-Whitney U test was used to compare mobility in each variant (* is p = 0.0124, *** is p = 0.8227).

a

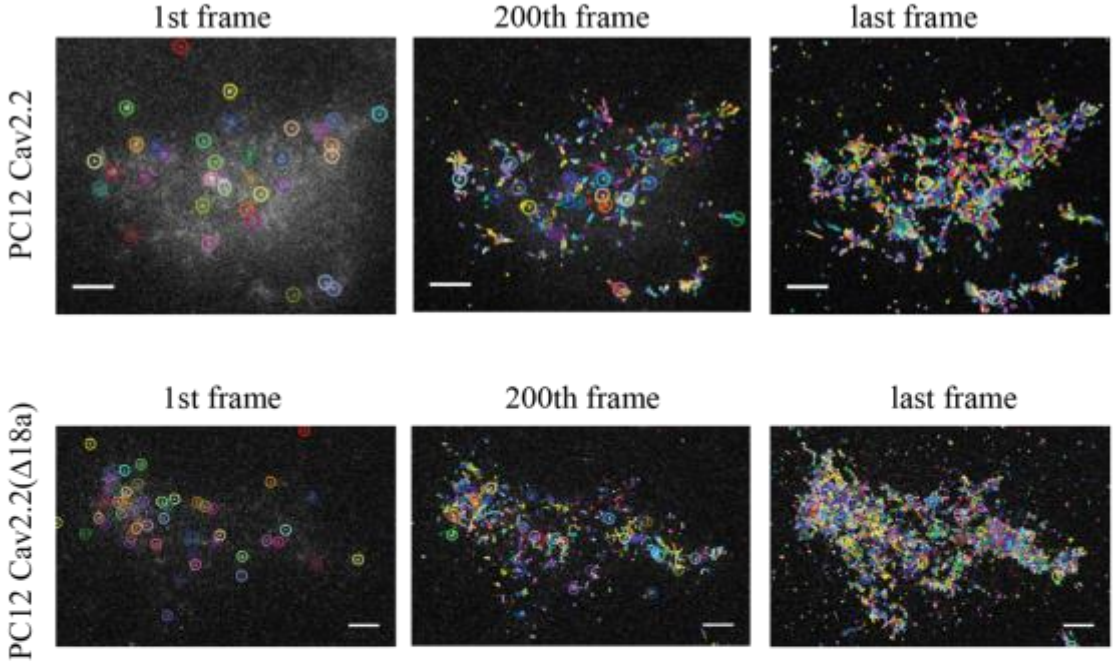

b

	Average speed (µm·s-1)		Min speed (µm·s-1)		Max speed (µm·s-1)	
	Cav2.2	Cav2.2(Δ18a)	Cav2.2	Cav2.2(Δ18a)	Cav2.2	Cav2.2(Δ18a)
Nr of cells	5	4	5	4	5	4
Nr of tracks	17589	21904	17589	21904	17589	21904
Minimum	3.207×10-5	1.408×10-5	3.239×10-5	2.702×10-5	6.414×10-5	2.816×10-5
Median	0.283	0.246	0.048	0.059	0.696	0.588
Maximum	1.837	1.755	0.719	0.833	4.430	5.228
Mean	0.305	0.273	0.059	0.067	0.751	0.655
SD	0.187	0.216	0.046	0.046	0.472	0.529

Figure 4.7 Single particle tracking of N-type calcium channels in PC12 cells. (a) Cav2.2/Cav2.2(Δ18a) c calcium channels were expressed with PACherry in HEK293 cells and analysed in Matlab with particle tracking software written by I. Schlangen. Images represent the detection in the 1st frame following with the tracking in the 200th and last frame. Each colour represents different particle (scale bar 5 µm) (b) Table with results of average, min and max speed for full-length (Cav2.2) and splice (Cav2.2(Δ18a)) calcium channels variant. Total number of frames = 4,000.

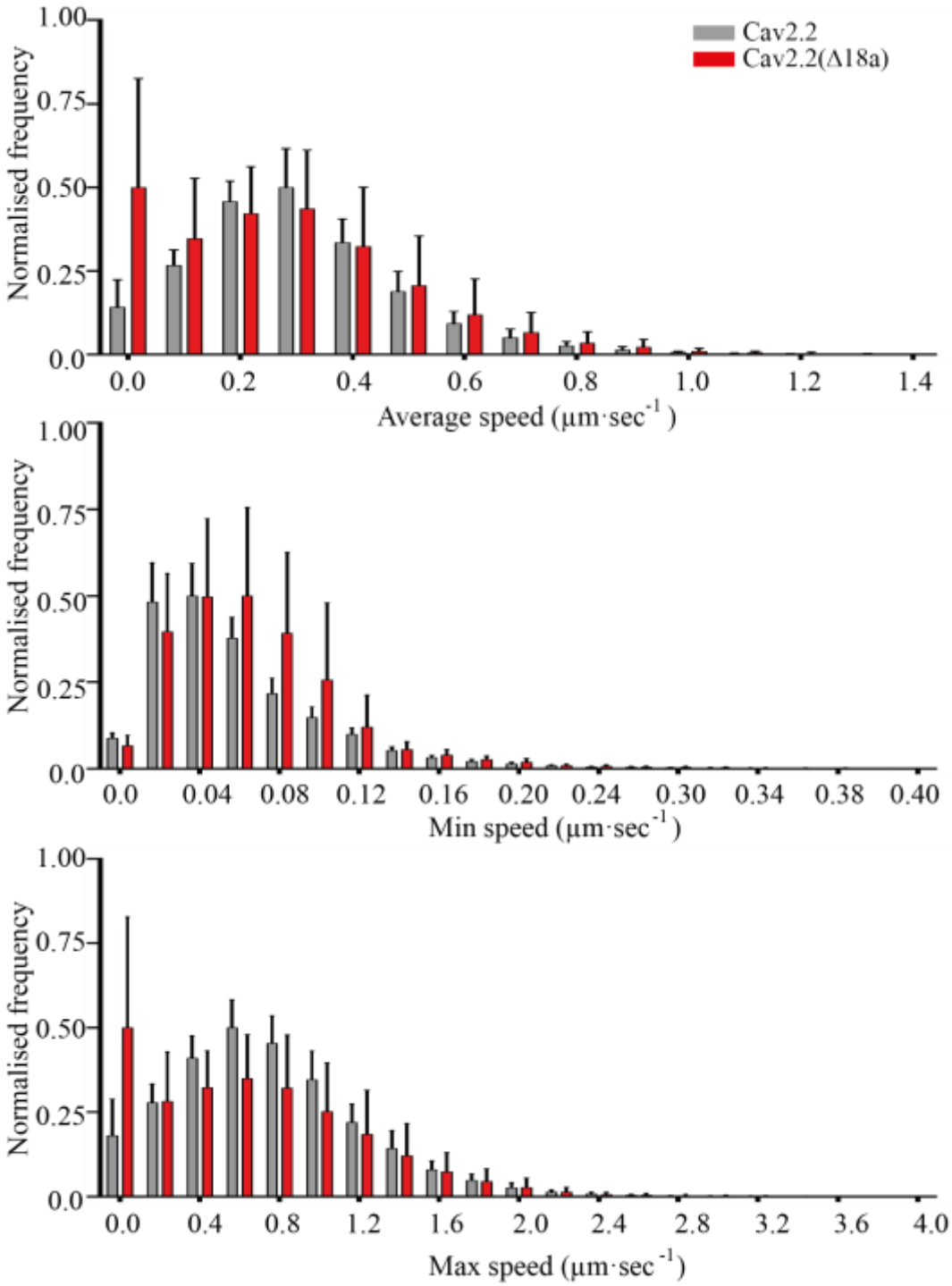

Figure 4.8 The mobility of N-type calcium channels in the PC12 cells. Combined average, min and max speed for each individual N-type calcium channel presented as the normalized frequency histogram of mean ± SD (number of tracks 17589 for Cav2.2, 21904 for Cav2.2(Δ18a)). The non-parametric Mann-Whitney U test was used to compared mobility in each variant (**** is $p < 0.0001$).

To check the difference in mobility between N-type calcium channels expressed in HEK293 and PC12 cells, the non-parametric Kruskal-Wallis was performed. There is a significant difference in average speed between two cell types but also between calcium channel variants (figure 4.9). The full-length N-type calcium channel variant is faster in PC12 than in HEK293 cells (figure 4.9). The opposite trend can be seen for N-type calcium channels without synprint motif. The Cav2.2(Δ18a) calcium channels in PC12 cell move slower than in the HEK293 cells (figure 4.9). Comparison of minimum speed showed no significant difference between full-length Cav2.2, however, there is a significant difference for the splice variant. The minimum speed is higher than in HEK293 cells (figure 4.9). The contrast in maximum speed can be also noted. There is a significant difference for both N-type calcium channel variant expressed in HEK293 and PC12 cells. The variant with synprint site moves faster in PC12 cells, while the variant without synprint motif is slower in the same cell type (figure 4.9).

To summarise the results, the N-type calcium channels without synprint site are more static than the full-length N-type calcium channels in both HEK293 and PC12 cells. The median speed of N-type calcium channels expressed in PC12 is higher than in HEK293 cells, nevertheless they maximum average movement is slower (1.8 $\mu m \cdot s^{-1}$) than in HEK293 cell (3.3 $\mu m \cdot s^{-1}$) (figure 4.9).

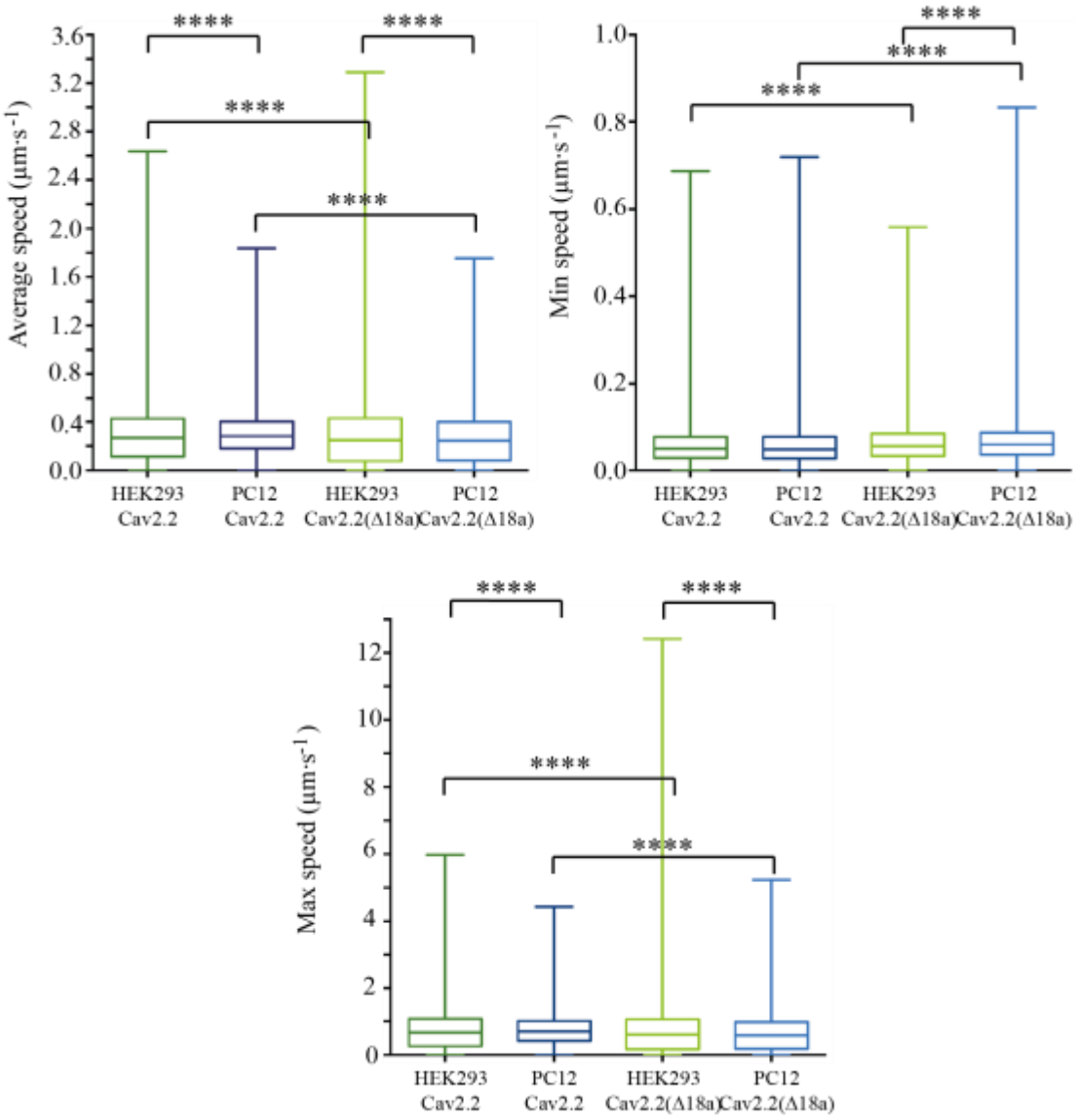

Figure 4.9 The comparison of N-type calcium channels mobility in HEK293 and PC12 cells. Boxplots of the average, min and max speed of Cav2.2/Cav2.2(Δ18a) calcium channels. Statistical significance was verified using the non-parametric Kruskal-Wallis test for multiple comparisons. The centre line indicates median value, the boxes 25th and 75th quartile values, and whiskers minimum and maximum values (**** = $p<0.0001$).

4.5 Conclusions

My studies suggest a close location of calcium channels to the vesicle-docking/release machinery[46]. This localisation may be explained by the direct interaction of SNARE proteins with voltage-gated calcium channels[55]. In this chapter, I wanted to answer the question about the interaction of N-type calcium channels with syntaxin-1A. Firstly, the interaction of those two proteins was tested with the FLIM-FRET technique. However, the results indicated no FRET efficiency, which may mean that Cav2.2 calcium channels and syntaxin-1A do not interact. FRET can be only detected when two fluorophores are in the close proximity, <10 nm[139]. The Ca^{2+} concentration needed for effective exocytosis which is around 100 μM can be found at 20 nm distance from the channel mouth[209]. Electron microscope and patch clamp data indicated also the sites of exocytosis even 100-200 nm outside of the individual calcium channel cluster[210]. Another thing that can have the influence on results is fluorophore orientation. Here the N-type channels with EGFP-tagged were expressed in cells and labelled with the antibody. However it is known that the EGFP is tagged to the C-terminus of α_{1B} subunit, the exact epitope for HPC-1 antibody has not been mapped. As I mentioned in conclusion in chapter 3, the fluorescent protein which has a size of ~4 nm[208]is linked to the protein of interest by a ~5 nm linker[208]. This additional distance can also affect the results. The solution for this would be immunolabeling both N-type calcium channels and syntaxin-1A, or expressing with the reliable pair of fluorescent proteins. Unfortunately, there is no good Cav2.2 calcium channel antibody commercially available for immunostaining to test the results.

My FLIM-FRET data demonstrated no close (<10 nm) interaction between N-type calcium channels and syntaxin-1A are supported by my nearest neighbour results. The number of syntaxin-1A molecules within different N-type calcium channel clusters size was analysed. Overall the majority of syntaxin-1A molecules within close proximity <25 nm is zero. The number of molecules increases with the distance. The statistical test of syntaxin-1A molecules number shows a significant difference between full-length and synprint site deletion N-type calcium channels. The number of syntaxin-1A is smaller for Cav2.2(Δ18a) variant. Previous research revealed[74] the occurrence of small and larger syntaxin-1A clusters at the PC12 cells cell membrane. Sieber et al.[72] demonstrated the existence of two different types of syntaxin-1A distribution; clustered and dispersed single molecules. It is

also thought that the probability of exocytosis increase with the appearance of syntaxin-1A clusters[164]. The results from nearest neighbour analysis may support this. When N-type calcium channels contain the synprint interaction site, the syntaxin-1A form clusters thus can bind to the channel mouth. While there is no synprint motif, syntaxin-1A takes single or smaller cluster configuration. To test this hypothesis, dual-colour single molecule imaging could have been done.

The last step in this chapter examines the mobility of N-type calcium channels in two different cell types, with (PC12 cells) or without (HEK293 cells) SNARE proteins. Overall the N-type calcium channels in the presence of SNARE proteins are more mobile. That can be explained by their role in the exocytosis machinery. Assuming the vesicles must be docked and fused in the close proximity to the calcium channels, that could clarify their higher mobility. There is also a significant difference between two variants of Cav2.2 calcium channels. The variant without the synprint motif is more static. This difference can be seen also between HEK293 and PC12 cells. This splice variant is less mobile in secretory cells, while the synprint interaction site is presence calcium channels are more mobile. My interpretation of these results is, the N-type calcium channels expressed in cells without SNARE proteins they are less mobile because they are not a part of the exocytosis machinery. When expressed in secretory cells, but lacking synprint interaction site, there is less probability the exocytosis occur and they are more static. The next step for this experiment would be the measurement of the single vesicle fusion[211] event for N-type calcium channels with and without synprint motif.